Rom J Morphol Embryol 2021, 62(3):713–721 ISSN (print) 1220–0522, ISSN (online) 2066–8279 doi: 10.47162/RJME.62.3.08

ORIGINAL PAPER

RJME Romanian Journal of Morphology & Embryology http://www.rjme.ro/

Hypertension induces compensatory left ventricular hypertrophy by a mechanism involving gap junction lateralization and overexpression of CD36, PKC and MMP-2

MĂDĂLINA DUMITRESCU, ALINA CONSTANTIN, ANDREEA MIRUNA NEMECZ, EMANUEL DRĂGAN, LUCIA DOINA POPOV, GABRIELA TANKO

Nicolae Simionescu Institute of Cellular Biology and Pathology of the Romanian Academy, Bucharest, Romania

Abstract

Hypertension-induced left ventricular hypertrophy evolves initially as an adaptive response meant to minimize ventricular wall stress. The mechanisms involved in the preservation of the cardiac function during the "compensatory" phase of the left ventricular hypertrophy are still unclear. Therefore, we aimed at uncovering fine changes that aid the heart to cope with the increased stress in hypertension. Male golden Syrian hamsters were given N^G-nitro-L-arginine methyl ester (L-NAME) for 16 weeks, and they became hypertensive (HT), developing left ventricular hypertrophy with no impaired contractility or fibrosis. As compared to age-matched control hamsters, the hypertrophied left ventricles in L-NAME-induced HT hamsters exhibited the following structural and molecular changes: (*i*) accumulation of lipid droplets (LDs) within cardiomyocytes and relocation of gap junctions to the lateral membrane of cardiomyocytes or close to mitochondria (revealed by electron microscopy); (*ii*) overexpression of the cluster of differentiation 36 (CD36) fatty acid transporter, protein kinase C (PKC), and matrix metalloproteinase-2 (MMP-2), enhanced activation of the phosphoinositide 3-kinase (PI3K)/protein kinase B (AKT) pathway, and unchanged expression of the connexin 43 (Cx43) and N-cadherin junctional proteins (assessed by Western blot); (*iii*) increased protein carbonyl content, assessed with a 2,4-Dinitrophenylhydrazine (DNPH)-based spectrophotometric assay, indicative of an enhanced reactive oxygen species (ROS) production; and (*iv*) augmented MMP-2 activity (determined by gelatin zymography). These changes may participate in an orchestrated adaptive hypertrophic growth response that helps to maintain cardiac performance, in HT hamsters. Together, these findings could provide support for designing future strategies meant to prevent the transition from compensatory left ventricular hypertrophy to decompensated heart failure.

Keywords: ventricular hypertrophy, experimental hypertension, gap junction, intramyocardial lipid droplets.

Introduction

Hypertension is a common condition leading to diabetes and cardiovascular diseases. Initially, in hypertension, left ventricular hypertrophy evolves as a compensatory adaptation meant to counterbalance the increase in ventricular wall stress. Over time, this adaptive hypertrophic response becomes maladaptive and leads to heart failure. However, the mechanisms enabling the cardiac function to be maintained in the compensatory phase of left ventricular hypertrophy are still not completely clear [1].

Cardiac contractile performance relies on the balance between energy demand and energy-yielding substrates. The healthy heart mainly uses long-chain fatty acids (FAs) as energy sources. The uptake of FAs into cardiomyocytes is mostly mediated by FA translocase [FAT/cluster of differentiation 36 (CD36); hereafter referred to as CD36] [2]. Upon entering the cardiomyocytes, most FAs undergo β-oxidation for energy production, or are esterified to triacylglycerols, which are temporary deposited in intracellular lipid droplets (LDs) [3]. Current data indicate that cardiac CD36 may primarily target FAs to β-oxidation; also, CD36 intervenes in FA transfer within mitochondria, and enhances FA esterification [4].

Nitric oxide (NO), a critical regulator of blood pressure, is actively involved in cardiac contraction, metabolism, and remodeling [5]. Animal models (such as rats or mice) obtained by blocking NO production with NO synthase (NOS) inhibitors, like N^G-nitro-L-arginine-methyl ester (L-NAME), have been used previously to study alterations taking place in hypertension [6].

Aim

In this study, we aimed at unravelling early modifications that accompany left ventricular hypertrophy in hypertension and choose to administer L-NAME to golden Syrian hamsters that, as reported, were successfully employed to investigate atherogenesis [7] or accelerated atherosclerosis in diabetes [8], on account of important similarities between hamsters and humans. Our study was conducted to identify structural and biochemical changes that could explain the heart adaptation to stress in hypertension induced-compensatory left ventricular hypertrophy.

Materials and Methods

The experimental model

Twenty-five male golden Syrian hamsters (*Mesocricetus*

auratus) 4-month-old, weighting ~120 g, were randomly divided into two experimental groups: (*1*) the hypertensive (HT), L-NAME-treated hamsters (45 mg/kg body weight, n=15) group, and (*2*) the controls, receiving saline solution (n=10; C group). The L-NAME, or the vehicle, was administered by gavage five times per week. After 16 weeks, the hamsters were subjected to hemodynamic evaluation (as described below), then euthanized, their hearts excised, and the left ventricles (LVs) rapidly harvested for further evaluation. The hamsters were housed under standard environmental conditions (12-hour light/dark cycle, at 23±2°C), with free access to water and rodent chow. Animal handling and experimental procedures were conducted in accordance with the European Commission Directive 86/609/EEC and the Guide for the Care and Usage of Laboratory Animals [US *National Institutes of Health* (NIH) Publication No. 85–23, revised 1996], and were approved by the local Ethics Committee of the Nicolae Simionescu Institute of Cellular Biology and Pathology of the Romanian Academy, Bucharest, Romania.

Blood pressure measurement

The arterial blood pressure was measured in anesthetized hamsters. Briefly, a catheter filled with heparinized saline was inserted into the abdominal aorta and linked to a MLT844 pressure transducer connected *via* a ML118 bridge amplifier to a PowerLab 4/30 data acquisition system running LabChart v.5.5 (AD Instruments, Oxford, UK). After 5-minute stabilization, data on blood pressure and heart rate were collected for 10 minutes and analyzed with the same software.

Blood and heart tissue collection

After blood pressure recording, blood samples were drawn from the aorta under deep anesthesia, then, the animals were perfused with oxygenated phosphate-buffered saline (PBS) through the abdominal aorta, using the punctured vena cava as outlet. The perfusion continued with a fixative solution for electron microscopy (see below), or the heart was rapidly excised, the LV blotted dry, weighted, snap-frozen in liquid nitrogen and stored at –80°C for Western blot and zymography assays. The levels of glucose, cholesterol, NOx (the stable end products of NO), and the activity of angiotensin-converting enzyme (ACE) were assessed in the blood samples. The ratio between the LV and the body weight (BW) was calculated as an index of left ventricular hypertrophy.

Biochemical determinations

Glucose and cholesterol concentrations were determined using diagnostic kits (Dialab GmbH, Austria). NOx levels were assessed using the Griess reagent [9], and the ACE activity was evaluated by fluorometric detection of histidyl–leucine (His–Leu) after hippuryl–His–Leu proteolysis to His–Leu and hippuric acid [10].

Western blot assay

LVs were homogenized in cold lysis buffer supplemented with a protease inhibitor cocktail (Roche, Mannheim, Germany) and Phenylmethylsulfonyl Fluoride. Lysates were centrifuged at 16 000×g (10 minutes at 4°C), and the supernatants were collected and stored at –80°C until use. Equal amounts of protein (~30 μg per lane) were loaded and separated on 8% or 10% Sodium Dodecyl Sulfate (SDS)–Polyacrylamide gel electrophoresis (PAGE), and electrotransferred onto Nitrocellulose membranes (Bio-Rad Laboratories). The latter were blocked with 5% (*w/v*) non-fat dry milk in Tris-buffered saline [100 mM Tris-HCl, pH 7.5, 150 mM Sodium Chloride (NaCl)] containing 0.05% Tween 20 for one hour and incubated overnight at 4°C with one of the following primary antibodies: anti-endothelial NOS (eNOS), anti-phospho-inositide 3-kinase (PI3K), anti-protein kinase B (AKT), anti-phospho-AKT (Ser473), anti-protein kinase C (PKC), anti-p53; anti-CD36, anti-connexin 43 (Cx43), anti-N-cadherin, anti-MMP-2, anti-MMP-9, and anti-β-actin (all from Santa Cruz Biotechnology, Heidelberg, Germany). The immunoreactive proteins were detected with the appropriate Horseradish Peroxidase (HRP)-conjugated secondary antibodies (rabbit or mouse; Santa Cruz Biotechnology, Heidelberg, Germany) using an enhanced chemiluminescence kit (Amersham Pharmacia Biotech, UK Ltd., Little Chalfont, Buckinghamshire, UK) and a LAS-4000 luminescent image analyzer (FUJIFILM, Tokyo, Japan). Bands intensities were quantified with TotalLab Quant software; β-actin served as loading control.

Detection of protein carbonyls

Protein-bound carbonyl groups were determined in left ventricular homogenates after derivatization of carbonyl moieties with 2,4-Dinitrophenyl-hydrazine (DNPH) to obtain stable hydrazone–protein adducts [11]. Protein carbonyl content was calculated from the peak absorbance of spectra at 360–385 nm, considering the molar absorption coefficient for aliphatic hydrazones (22 000 $M^{-1}cm^{-1}$). The results were expressed as nmols carbonyl per mg of protein.

Transmission electron microscopy

Under deep anesthesia, hamsters were perfused through the abdominal aorta first with oxygenated PBS, and then with a mixture of 2.5% Glutaraldehyde and 1.5% Paraformaldehyde in 0.1 M Sodium Cacodylate buffer, pH 7.2, with 2.5 mM Calcium Chloride ($CaCl_2$), for 10 minutes. Small fragments of the LVs (~1 mm^3) were collected and processed for routine electron microscopy. Briefly, the samples were post-fixed in 1% Osmium Tetroxide in 0.1 M Sodium Cacodylate buffer (90 minutes at 4°C), stained *en bloc* with 0.5% Uranyl Acetate, dehydrated through a graded series of Ethanol, cleared in Propylene Oxide, and embedded in Epon 812 resin. Ultrathin (~70–80 nm) sections were double stained with Uranyl Acetate and Lead Citrate and examined under a Tecnai G2 Spirit BioTwin electron microscope (FEI Company, Eindhoven, Netherlands) at 100 kV. Images were captured with a MegaView III TEM charge coupled device (CCD) camera (Olympus Soft Imaging Solutions GmbH, Münster, Germany).

Assays for matrix metalloproteinase (MMP)-2 and MMP-9 activity

The gelatinolytic activities of MMP-2 and MMP-9 were evidenced by zymography, performed on 7.5% SDS–PAGE co-polymerized with 1% Gelatin (*w/v*), under non-reducing conditions [12]. Gels were washed twice

in 2.5% Triton X-100 (to remove SDS) and incubated in developing buffer (50 mM Tris-HCl, pH 7.5, 5 mM $CaCl_2$, 0.2 M NaCl, and 0.02% Brij-35) overnight at 37°C. After staining with Coomassie Blue R250, the proteolytic activity was revealed by the clear bands against a blue background. Gelatinolytic signals were quantified by reverse-image densitometry, and the results were reported as percentages of control.

Statistical analysis

Data are presented as mean ± standard error of the mean (SEM) unless otherwise stated. To determine statistical significance between HT and C groups, data were analyzed using Student's *t*-test. *p*-values of 0.05 or less were considered significant.

Results

Characterization of L-NAME-induced HT hamster model

The morphological, physiological, and biochemical characteristics of the HT and control hamsters are shown in Table 1.

Table 1 – ***Morphological, physiological and biochemical characteristics of hamster groups***

	C group (*n*=10)	HT group (*n*=15)
BW [g]	103.6±12.3	116.4±12.8*
LVW [mg]	319.9±15.3	445.1±19.9*
LVW/BW [mg g^{-1}]	3.09±0.11	3.85±0.17*
Heart rate [beats min^{-1}]	321.4±6.2	390.4±2.3*
P [mmHg]	83±1.6	158±5.5*
dP/*dt* max [mmHg s^{-1}]	1922.2±235.2	3268.3±84.8*
dP/*dt* min [mmHg s^{-1}]	841.2±16.7	1433.8±176.6
NOx [µmol L^{-1}]	21.3±2.1	9.5±1.8*
Blood glucose [mg dL^{-1}]	65.7±5.5	58.6±4.2
Serum cholesterol [mg dL^{-1}]	118.06±6.7	108.6±5.8
Serum ACE activity [nmol His–Leu mL^{-1} min^{-1}]	28.06±4.8	34.8±4.4

ACE: Angiotensin-converting enzyme; BW: Body weight; C: Control; His–Leu: Histidyl–leucine; HT: N^G-nitro-L-arginine-methyl ester (L-NAME)-induced hypertensive animals; LVW: Left ventricular weight; *n*: No. of animals; P: Mean arterial pressure; *dP*/*dt*: Rate of change (rise or decline) of pressure with respect to time. Values are expressed as means ± standard error of the mean (SEM); **p*<0.05 *vs.* C group.

Compared to controls, the hamsters treated for 16 weeks with L-NAME manifested a significantly higher blood pressure (~90%) and heart rate (~21%; $p<0.05$ *vs.* C group). BW and the LV weight of the HT hamsters were greater than that of control animals (by ~25%; $p<0.05$). Moreover, the ratio between the LV weight and the BW was markedly increased in HT group ($p<0.05$ *vs.* C group), an indicative of left ventricular hypertrophy. In addition, the increased rates of pressure rise and decline (*dP*/*dt* max; *dP*/*dt* min; by ~70%) in HT hamsters ($p<0.05$ *vs.* C group) were suggestive of an adaptive, enhanced contractility of the heart in HT animals. It is worth mentioning that the average rate of blood pressure changes normalized to mean pressure [(*dP*/*dt*)/*P*] was similar in both groups (16.7 s^{-1} for HT, and 17 s^{-1} for C group, respectively), denoting that in HT hamsters the heart maintained its contractile function. The ACE activity was only slightly increased in HT hamsters ($p>0.05$ *vs.* C group) implying that our HT animal model was less dependent on the renin–angiotensin system activation than other models [13]. As expected, the serum NOx levels in HT hamsters were diminished (by ~45%; $p<0.01$ *vs.* C group), confirming the inhibition of NO production by L-NAME. Moreover, Western blot assays showed that the mean level of eNOS expression was comparable between the two experimental groups, signifying that NO deficiency resulted from the reduced eNOS activity rather than the eNOS protein down-regulation. Circulating glucose and cholesterol levels were comparable between the two groups, indicating that the administration of L-NAME did not affect glucose or cholesterol metabolism. There was no significant difference in mortality rate between HT and C groups (data not shown).

Ultrastructural changes of hypertension-induced hypertrophic LV of hamsters

Electron microscopic examination revealed that the left ventricular structure in HT hamsters was in general similar to that in controls. The sarcomeres were regularly aligned, and neither excessive deposition of extracellular matrix (ECM) (fibrosis) that would hamper normal conduction, nor infiltrating cells between cardiomyocytes were detected in HT hamsters (Figures 1A and 2A). Of note, cardiomyocytes in the LVs of HT hamsters were endowed with numerous intermyofibrillar mitochondria (Figures 1A and 2A), and exhibited an abundance of LDs, in-between the myofibrils or close to mitochondria (Figure 1, A and B; Figure 2, A, B, and D). In addition, numerous intracellular glycogen stores were present in ventricular cardiomyocytes of HT hamsters (Figure 1B), probably as an alternative energy substrate, so as to meet high energy demands for maintaining cardiac contractility. Assuming that accumulation of LDs could be due to an enhanced FAs uptake within the cardiomyocytes, we searched for the expression of the FA transport protein, CD36, in the LV homogenates. Western blot assay revealed that CD36 protein was overexpressed in the LVs of HT hamsters, as compared to controls (Figure 1C; $p<0.05$).

It is well-known that cardiomyocytes are connected *via* complex junctional complexes that facilitate cell-to-cell coupling [14]. Examination of these coupling junctions in the hypertrophied ventricles of HT hamsters revealed that numerous gap junctions (Gjs) were displaced from their typical location at the level of the intercalated discs (IDs) and relocated either to the lateral membrane of cardiomyocytes (Gj "lateralization") or near the mitochondria (Figure 2, A–D). In conjunction with this structural observation, we evaluated the protein expression of Cx43, the main Gj protein, and N-cadherin, an adherens junctional molecule instrumental in maintaining Cx43 within the IDs [15], and we found no significant differences in Cx43 and N-cadherin expression levels in the LVs from HT and C hamsters (Figure 2E). These results were in line with the lack of electrical conduction abnormalities in L-NAME-induced HT hamsters.

PI3K/AKT pathway is activated in the LVs of HT hamsters

The phosphoinositide 3-kinase (PI3K)/AKT signaling pathway plays critical roles in hypertrophic growth and survival of cardiomyocytes in physiological or pathological conditions [16]. Therefore, we assessed the expression levels of PI3K and phospho-AKT (Ser473) in homogenates of LVs from HT and control hamsters. Western blot analysis showed that the expression level of the p85 subunit of PI3K was increased by ~2.3 fold (p<0.05 *vs.* C group), and the expression of phospho-AKT (Ser473) was ~1.5 fold higher (p<0.05) than in controls (Figure 3, A and B). These data provided evidence for a consistent activation of PI3K/AKT pathway in our HT model.

The hypertrophic LVs of HT hamsters exhibit a significant increased expression of protein carbonyls and PKC

Chronic NO deficiency facilitates excessive reactive oxygen species (ROS) generation, which may drive cardiac phenotypic changes [17]. To address ROS production by hypertrophied ventricles of HT hamsters, we evaluated the protein carbonyl content and the expression levels of redox-sensitive PKC and p53. The results showed that the carbonyl groups content was ~2.5-fold higher in the LV homogenates of HT hamsters than in controls (p<0.05), and the PKC was overexpressed by ~2.5-fold (p<0.05 *vs.* C group) (Figure 4, A and B). The protein expression level of p53, a key regulator of apoptosis, exhibited no significant differences between controls and HT hamsters (Figure 4C). Together, the overexpression of the redox-sensitive PKC and the lack of activation of the apoptotic pathway may have a contributory role in sustaining cardiac function in L-NAME-induced hypertension.

The hypertrophic LVs of HT hamsters display increased expression and activity of MMP-2

MMPs activation is a critical step in cardiac remodeling, often promoted by increased ROS production. Examination of the protein expression and activation of MMP-2 and MMP-9 by Western blot and zymography revealed that the protein expression of MMP-2 was increased by ~1.5-fold, and its gelatinolytic activity was ~2.5-fold higher in the LVs of HT hamsters, compared to controls (p<0.05; Figure 5, A and B), while no significant changes were found in MMP-9 protein expression and activation between HT and C groups (Figure 5, A and B). These results suggested a potential involvement of MMP-2 in the compensatory hypertrophic response in L-NAME-induced HT hamsters, while MMP-9 appeared not to be active to initiate harmful events.

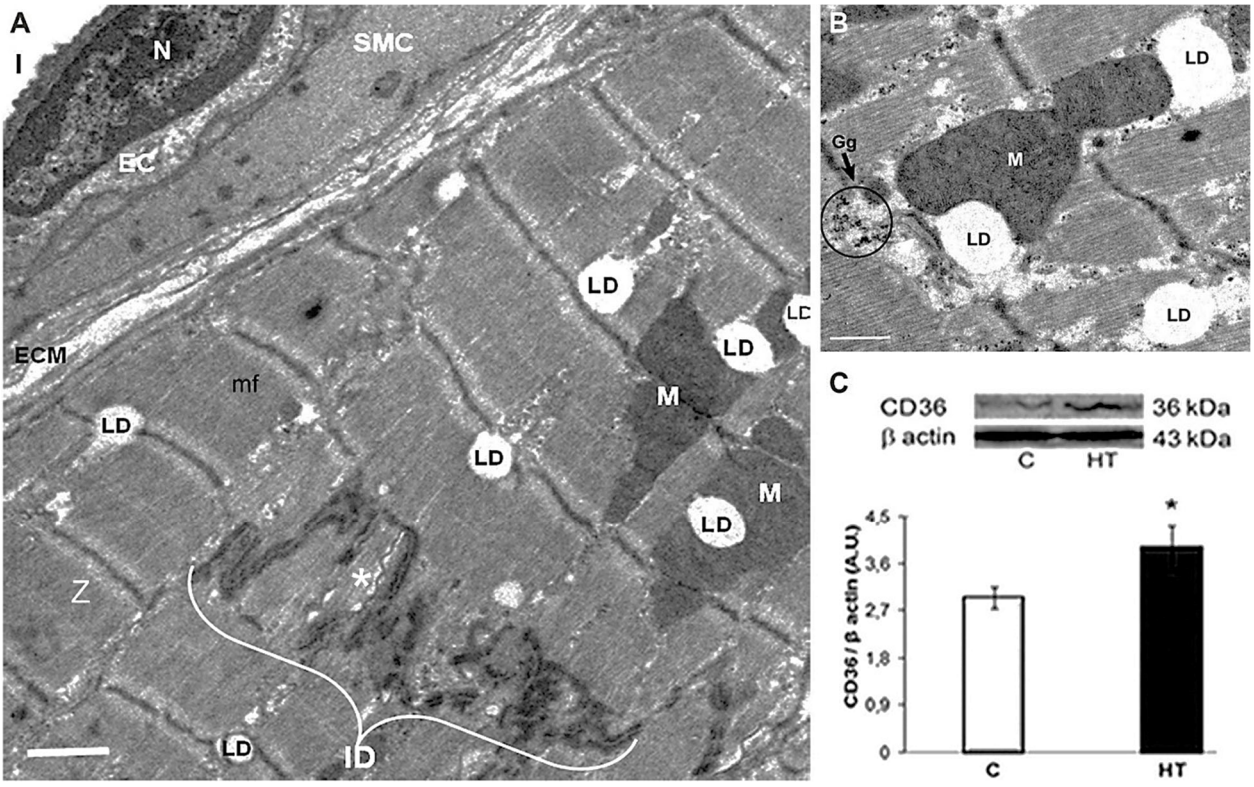

Figure 1 – ***LV of a HT hamster with compensatory myocardial hypertrophy: (A and B) TEM revealing the apparent normal structure of a cardiomyocyte with regular arrangement of mf and Z. Note in (A) the abundance of LD, often at the level of Z, associated with M or adjacent to an ID that encloses a long, ribbon-shaped Gj (asterisk), and in (B) the proximity between M, LD and Gg. Scale bar: (A) 1 µm; (B) 0.5 µm; (C) CD36 protein expression in the LV homogenate is significantly increased compared to controls [C]. Representative immunoblots (upper panel) and the densitometric analysis of the bands expressed as AU are shown. The intensities of the bands were quantified with TotalLab Quant software. β-Actin served as protein loading control. n: 3–4 hamsters in each group. *p<0.05 vs. [C] group. AU: Arbitrary units; CD36: Cluster of differentiation 36; EC: Endothelial cell; Gg: Glycogen granules; Gj; Gap junction; HT: Hypertensive; ID: Intercalated disc; l: Capillary lumen; LD: Lipid droplets; LV: Left ventricle; M: Mitochondria; mf: Myofibrils; N: Nucleus; SMC: Smooth muscle cell; TEM: Transmission electron microscopy; Z: Z-lines.***

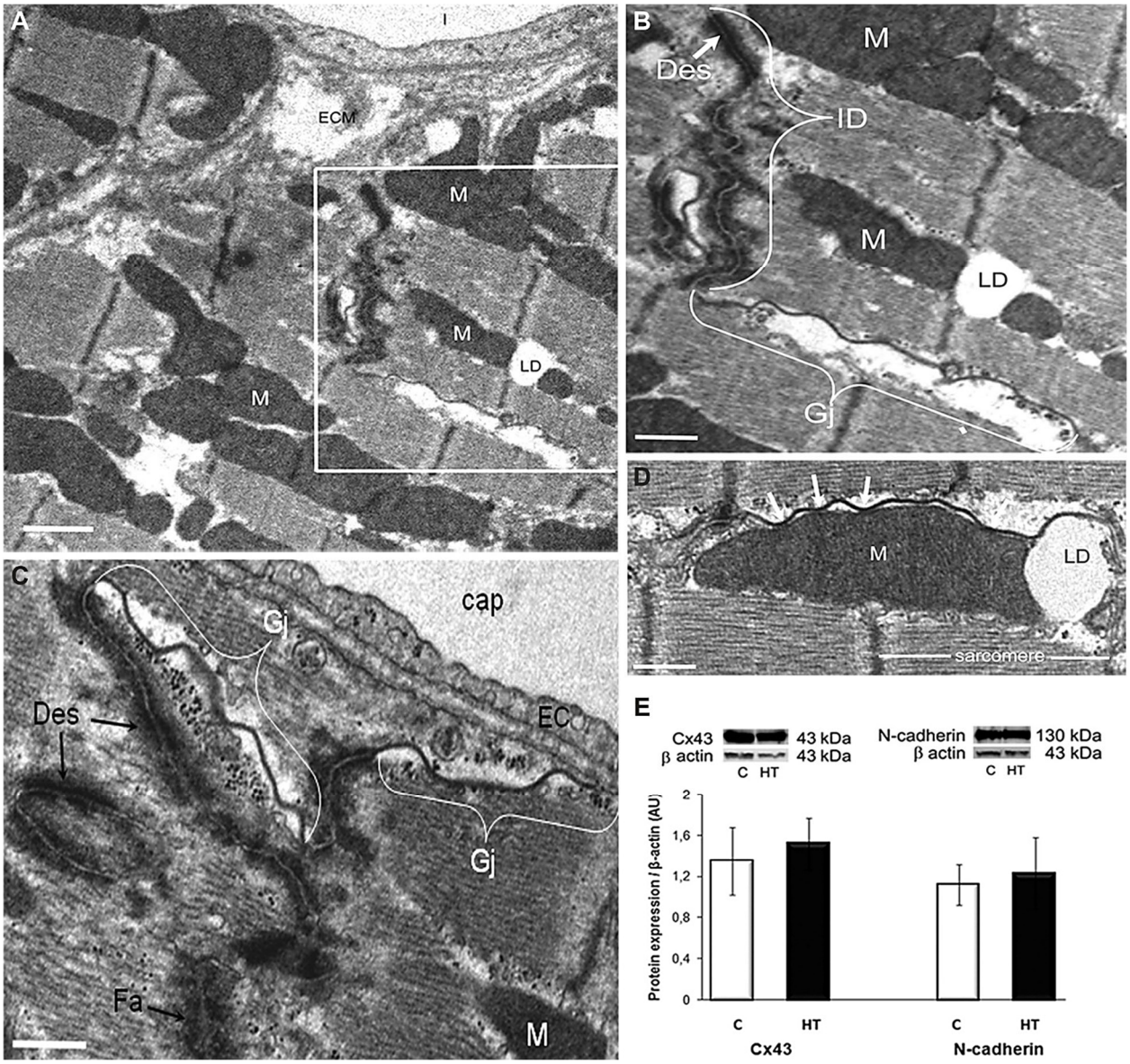

Figure 2 – ***The architecture of the IDs between cardiomyocytes in the LV of a HT hamster with compensatory cardiac hypertrophy is slightly modified, whereas the expression of Cx43 and N-cadherin junctional proteins remains unchanged, as compared to controls [C]: (A and B) Electron micrographs highlighting an ID, and Gj redistribution to the lateral membrane of cardiomyocyte (lateralization). An enlarged view of the boxed area in (A) is shown in (B). Scale bar: (A and B) 1 µm; (C and D) Electron micrographs representative for lateralized Gjs that associate with electron-dense structures with the morphology of Des and Fa in (C), or in close connection with an interfibrillar M (white arrows) and its adjoining LD in (D). Scale bar: (C and D) 0.5 µm; (E) Representative immunoblots and densitometry of the bands (AU) revealing no differences in the expression of Cx43 and N-cadherin in the LV homogenates in HT and [C] hamsters. β-Actin was used as protein loading control. n: 3–4 hamsters in each group. AU: Arbitrary units; cap: Capillary; Cx43: Connexin 43; Des: Desmosomes; EC: Endothelial cell; Fa: Fascia adherens; Gj; Gap junction; HT: Hypertensive; ID: Intercalated disc; LD: Lipid droplet; LV: Left ventricle; M: Mitochondria; mf: Myofibrils.***

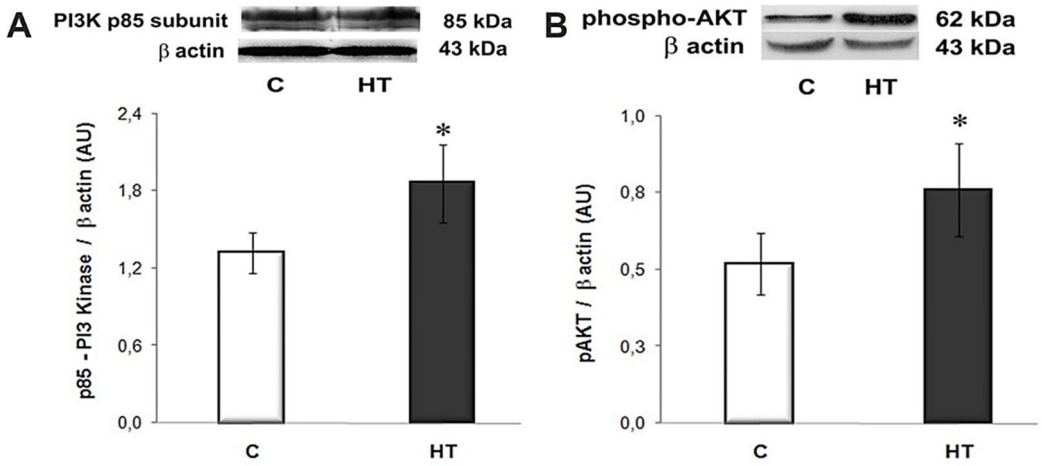

Figure 3 – ***The expression levels of PI3K (p85 subunit) (A) and phospho-AKT (Ser473) (B) are significantly increased in the LVs of HT hamsters compared to controls [C] and assessed by Western blot. Representative immunoblots and the densitometric analysis (AU) are displayed in the upper and lower panels, respectively. β-Actin was used as protein loading control. n: 3–4 hamsters in each group. *p<0.05 vs. [C] group. AKT: Protein kinase B; AU: Arbitrary units; HT: Hypertensive; LV: Left ventricle; PI3K: Phosphoinositide 3-kinase.***

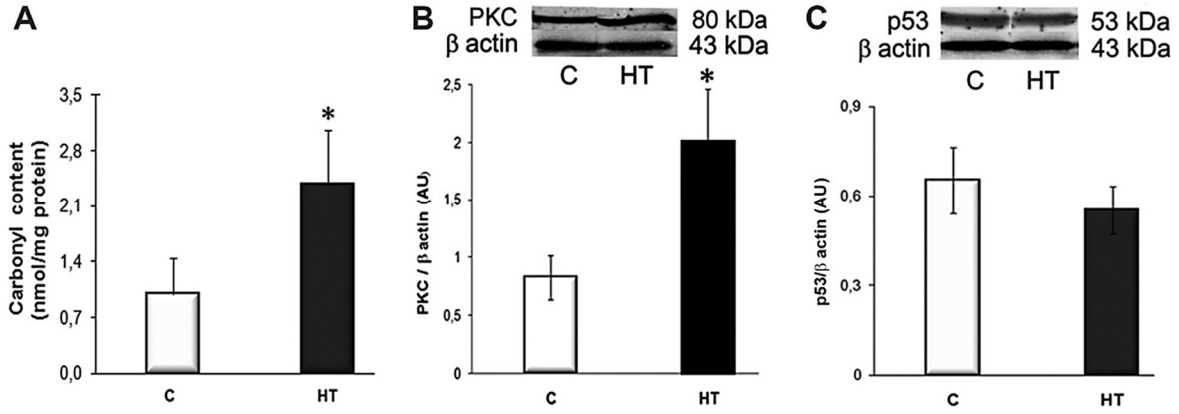

Figure 4 – ***Assessment of the ROS production in the LVs of HT hamsters by determining the protein carbonyl content and the expression levels of redox-sensitive PKC and p53: (A) Protein carbonyl content, assessed with a DNPH-based spectrophotometric assay, is significantly higher in homogenates of HT hamsters than in control [C] ones; (B and C) As compared to [C], the protein expression of PKC is significantly increased, whereas the expression of p53 is unchanged in HT hamsters. Representative Western blots and quantification of the bands' intensities (AU) are shown in the upper and lower panels, respectively. β-Actin was used as protein loading control. n: 3–4 hamsters in each group. *p<0.05 vs. [C] group. AU: Arbitrary units; DNPH: 2,4-Dinitrophenylhydrazine; HT: Hypertensive; LV: Left ventricle; PKC: Protein kinase C; ROS: Reactive oxygen species.***

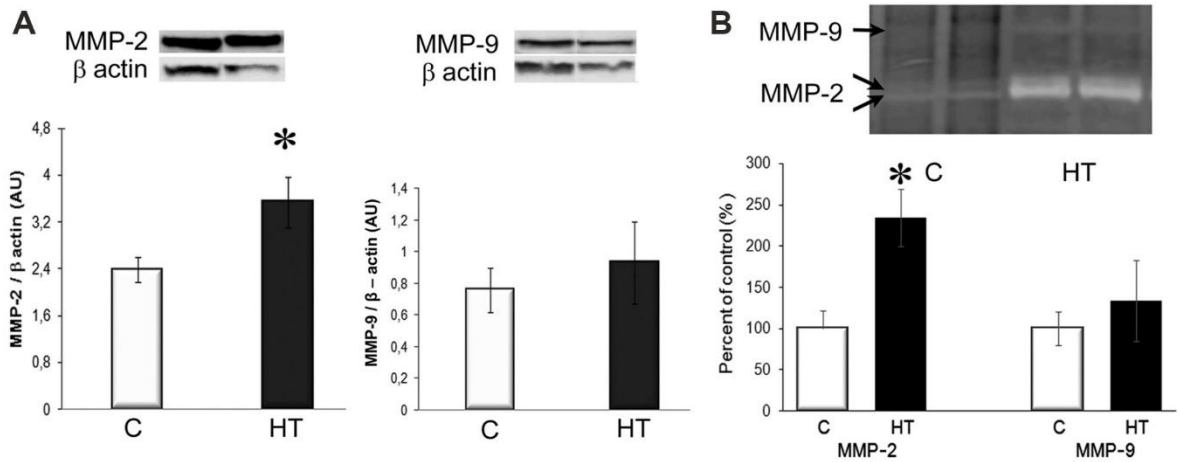

Figure 5 – ***MMP-2 protein expression and gelatinolytic activity significantly increased in the hypertrophic LV of HT hamsters: (A) MMP-2 and MMP-9 protein expression. Representative immunoblots (top) and the densitometric analysis (bottom) of the bands intensities, expressed as AU; (B) Gelatin zymography indicating an increased proteolytic activity of MMP-2 in HT hamsters. β-Actin was used as protein loading control. n: 3–4 hamsters in each group. *p<0.05 vs. [C] group. AU: Arbitrary units; [C]: Control; HT: Hypertensive; LV: Left ventricle; MMP: Matrix metalloproteinase.***

Discussions

Initially, hypertension-induced left ventricular hypertrophy compensates the increase in the hemodynamic load, and enhanced contractility is essential in maintaining cardiac function against the augmented wall stress [18]. However, the molecular changes and pathways underlying the adaptive LV hypertrophy are still unclear. Therefore, we examined several structural and biochemical aspects of the compensatory left ventricular hypertrophy in hamsters rendered HT by L-NAME treatment. The novel findings reported herein show that, in HT, the hypertrophic LVs exhibit: (*i*) an accumulation of LDs in cardiomyocytes and Gj lateralization; (*ii*) an increased protein expression of the FA transporter, CD36, and activation of the PI3K/AKT pathway; (*iv*) enhanced protein expression of redox-sensitive PKC, and (*v*) increased protein expression and activity of MMP-2. Together, these changes may constitute adaptations of the LV to high blood pressure so as to assist the heart in maintaining an appropriate contractile function.

The chronically L-NAME-treated animals have been previously shown to develop cardiac fibrosis [19]; however, in our HT hamster model, the LV did not display excessive interstitial or perivascular ECM deposition (Figures 1A and 2A). This discrepancy may arise from the different experimental model employed (mice *vs.* hamsters in our experiment) or the different time points examined.

The cardiomyocytes are metabolically flexible, using FAs or glucose to respond efficiently to environmental stimuli [20]. Alterations in FAs oxidation or triacylglycerols turnover rates may generate cytotoxic levels of lipid intermediates in hypertrophied or failing heart. However, the enhanced triacylglycerol turnover rate has been reported to be protective in several models of cardiac stress [21]. Growing evidence also points to LDs functioning not only as lipid stores but also as dynamic regulators of the cellular response to metabolic stress [22]. The abundance of LDs within cardiomyocytes, often located adjacent to mitochondria (Figure 1, A and B; Figure 2, A, B, and D) was a characteristic feature of the HT hamsters, and this location suggests an adaptation for eased delivery of LDs-packed triacylglycerols to the sites of adenosine triphosphate (ATP) production, so as to handle the high energy demand of the contracting myocardium.

Lipid accumulation is associated with increased expression of genes for FA-transport proteins, such as CD36 [23]. In HT hamsters, the overexpression of CD36 (Figure 1C) may indicate an intensified FAs uptake in cardiomyocytes within the hypertrophic LVs, as compared to controls. Worth mentioning, a common event in both contraction-induced FA transport and CD36 translocation is the AKT activation [24]. Likewise, the AKT activation and CD36 overexpression may participate in a synergic manner in the adaptive stress response in the LVs of HT hamsters. In addition, the abundant glycogen stores within cardiomyocytes of HT hamsters (Figure 1B) stand for the ability of the heart to use various substrates during compensatory hypertrophy, which is essential to produce adequate amount of ATP.

In the adult heart, cardiomyocytes are interconnected by IDs, *i.e.*, specialized junctional complexes responsible for maintaining cardiac tissue structure integrity and allowing synchronized contraction. At the ID, Cx43 forms Gjs that are responsible for electrical propagation. In pathological conditions, several Gjs relocate from the IDs to the lateral side of cardiomyocytes (Gj "lateralization"). In general, Cx43 expression appears to be unaltered or upregulated during the compensatory phase of hypertrophy, and diminished when hypertrophy becomes maladaptive, progressing to heart failure [25]. In the HT hamster model, we found numerous Gjs distributed on the lateral membranes of cardiomyocytes and/or in the vicinity of mitochondria (Figure 2, A–D), and the close proximity between Gjs and adjacent mitochondria may provide multiple sites for facilitated ions exchange between extracellular space and mitochondria [26]. Besides, the lack of significant differences in the expression of Cx43 and N-cadherin between HT and control hamsters (Figure 2E) may be in accordance with Seidel's hypothesis, which postulates that Gj lateralization could evolve to balance cardiac inhomogeneity, and to preserve electrical coupling when molecular organization of IDs is disturbed [27]. Moreover, aside from its growth-promoting effects, AKT activation may be involved in sustaining contractility of the LVs in HT. Previous reports suggested that AKT may increase Cx43 hemichannel levels at cell membranes and modulate Ca^{2+} handling and contractility in cardiac myocytes [28, 29].

Although enhanced contractility stimulates cardiac ROS formation, there are several features to withstand oxidative stress in compensatory cardiac hypertrophy [30]. ROS activate several redox-sensitive pathways, including PKC signaling. In our experiments, the enhanced protein carbonyl content in LVs of HT hamsters (Figure 4A) points to an increased ROS production. The overexpression of PKC (Figure 4B) is potentially related to the regulation of cardiac contraction [31], while the slightly diminished expression of p53 (Figure 4C) could be related, at least in part, to AKT activation, as AKT enhances murine double minute 2 (MDM2)-mediated ubiquitination and degradation of p53 [32].

One of the mechanisms linking ROS and cardiac hypertrophy implies the activation of MMP-2 and MMP-9, two key players in ECM turnover and myocardial remodeling [33]. The increased MMPs activity is usually considered detrimental in the HT heart, but in certain circumstances, MMP-2 may play a cardioprotective role. For instance, HT mice lacking MMP-2 develop cardiac hypertrophy and fibrosis earlier and to a greater extent [34]. A large body of evidence reveals that MMP-2, aside from degrading ECM proteins, also cleaves intracellular targets in the contractile machinery of cardiomyocytes, such as troponin I, myosin light chains, or α-actinin [35]. It is conceivable to consider that, by binding and cleaving sarcomeric proteins, MMP-2 may be involved in adding new sarcomeres during hypertrophic growth, and we can assume that the enhanced MMP-2 expression and activity in HT hamsters (Figure 5, A and B) may participate in myocardial contractility. As regards MMP-9, evidence incriminates its activation as being a causative factor for the left ventricular dysfunction [36]. Also, MMP-9 proteolytically degrades CD36 [37]. In the case of HT hamsters, left ventricular expression and activity of

MMP-9 were rather unchanged, as compared to controls (Figure 5, A and B), so MMP-9 neither decreased CD36 expression, nor exerted other negative effects on cardiac function at the time of the adaptive response.

Conclusions

In the initial adaptive stage of hypertension, the LV undergoes (*i*) an accumulation of LDs by a mechanism possibly involving the FA transporter, CD36, (*ii*) Gj lateralization without significant changes in Cx43 protein expression, (*iii*) enhanced ROS formation, and activation of MMP-2. These changes that represent adaptations of the LV to high blood pressure can sustain the proper functioning of the heart in stressful conditions. Cardiac LDs, as a source of fuel delivery, may balance the fluctuations in the metabolic demands. The redox-driven events and/or other mechanisms by which MMP-2 could indirectly improve contraction are likely to sustain the adaptation to stress of the hypertension-induced hypertrophied LV.

Taken together, these data provide support for future strategies targeted to prevent the transition from compensatory left ventricular hypertrophy to decompensated heart failure.

Conflict of interests

The authors declare that there is no conflict of interests.

Acknowledgments

The authors are thankful to Dr. Maya Simionescu for helpful interpretation of the results and presentation in this paper. We also acknowledge the valuable technical assistance of Marilena Isachi, Marcela Toader, Marilena Misici, and Safta Nae. This research was funded by the European Regional Development Fund through the Competitiveness Operational Program 2014–2020 (Grant No. POC-A.1-A.1.1.4-E-2015, ID: P_37_668; DIABETER), by the Romanian National Authority for Scientific Research, CNCS–UEFISCDI, through the projects PN-III-P1-1.2-PCCDI-2017-0527 and PN-III-P1-1.2-PCCDI2017-0797, and by the Romanian Academy.

References

[1] Saheera S, Krishnamurthy P. Cardiovascular changes associated with hypertensive heart disease and aging. Cell Transplant, 2020, 29:963689720920830. https://doi.org/10.1177/0963689720920830 PMID: 32393064 PMCID: PMC7586256

[2] Habets DDJ, Coumans WA, Voshol PJ, den Boer MAM, Febbraio M, Bonen A, Glatz JFC, Luiken JJFP. AMPK-mediated increase in myocardial long-chain fatty acid uptake critically depends on sarcolemmal CD36. Biochem Biophys Res Commun, 2007, 355(1):204–210. https://doi.org/10.1016/j.bbrc.2007.01.141 PMID: 17292863

[3] Heier C, Haemmerle G. Fat in the heart: the enzymatic machinery regulating cardiac triacylglycerol metabolism. Biochim Biophys Acta, 2016, 1861(10):1500–1512. https://doi.org/10.1016/j.bbalip.2016.02.014 PMID: 26924251

[4] Abumrad NA, Goldberg IJ. CD36 actions in the heart: lipids, calcium, inflammation, repair and more? Biochim Biophys Acta, 2016, 1861(10):1442–1449. https://doi.org/10.1016/j.bbalip.2016.03.015 PMID: 27004753 PMCID: PMC4983248

[5] Simon JN, Duglan D, Casadei B, Carnicer R. Nitric oxide synthase regulation of cardiac excitation–contraction coupling in health and disease. J Mol Cell Cardiol, 2014, 73:80–91. https://doi.org/10.1016/j.yjmcc.2014.03.004 PMID: 24631761

[6] Ribeiro MO, Antunes E, de Nucci G, Lovisolo SM, Zatz R. Chronic inhibition of nitric oxide synthesis. A new model of arterial hypertension. Hypertension, 1992, 20(3):298–303. https://doi.org/10.1161/01.hyp.20.3.298 PMID: 1516948

[7] Nistor A, Bulla A, Filip DA, Radu A. The hyperlipidemic hamster as a model of experimental atherosclerosis. Atherosclerosis, 1987, 68(1–2):159–173. https://doi.org/10.1016/0021-9150(87)90106-7 PMID: 3689479

[8] Simionescu M, Popov D, Sima A. Cellular and molecular alterations in diabetes-induced cardiovascular complications studied in an original experimental model. In: Cheţa DM (ed). New insights into experimental diabetes. Romanian Academy Publishing House, Bucharest, Romania, 2002, 173–209. https://www.worldcat.org/title/new-insights-into-experimental-diabetes/oclc/51934648

[9] Granger DL, Taintor RR, Boockvar KS, Hibbs JB Jr. Measurement of nitrate and nitrite in biological samples using nitrate reductase and Griess reaction. Methods Enzymol, 1996, 268:142–151. https://doi.org/10.1016/s0076-6879(96)68016-1 PMID: 8782580

[10] Oliveira EM, Santos RAS, Krieger JE. Standardization of a fluorimetric assay for the determination of tissue angiotensin-converting enzyme activity in rats. Braz J Med Biol Res, 2000, 33(7):755–764. https://doi.org/10.1590/s0100-879x2000000700005 PMID: 10881050

[11] Levine RL, Garland D, Oliver CN, Amici A, Climent I, Lenz AG, Ahn BW, Shaltiel S, Stadtman ER. Determination of carbonyl content in oxidatively modified proteins. Methods Enzymol, 1990, 186:464–478. https://doi.org/10.1016/0076-6879(90)86141-h PMID: 1978225

[12] Hadler-Olsen E, Kanapathippillai P, Berg E, Svineng G, Winberg JO, Uhlin-Hansen L. Gelatin *in situ* zymography on fixed, paraffin-embedded tissue: zinc and ethanol fixation preserve enzyme activity. J Histochem Cytochem, 2010, 58(1):29–39. https://doi.org/10.1369/jhc.2009.954354 PMID: 19755718 PMCID: PMC2796612

[13] Takemoto M, Egashira K, Usui M, Numaguchi K, Tomita H, Tsutsui H, Shimokawa H, Sueishi K, Takeshita A. Important role of tissue angiotensin-converting enzyme activity in the pathogenesis of coronary vascular and myocardial structural changes induced by long-term blockade of nitric oxide synthesis in rats. J Clin Invest, 1997, 99(2):278–287. https://doi.org/10.1172/JCI119156 PMID: 9005996 PMCID: PMC507795

[14] Zhao G, Qiu Y, Zhang HM, Yang D. Intercalated discs: cellular adhesion and signaling in heart health and diseases. Heart Fail Rev, 2019, 24(1):115–132. https://doi.org/10.1007/s10741-018-9743-7 PMID: 30288656

[15] Wei CJ, Francis R, Xu X, Lo CW. Connexin43 associated with an N-cadherin-containing multiprotein complex is required for gap junction formation in NIH3T3 cells. J Biol Chem, 2005, 280(20):19925–19936. https://doi.org/10.1074/jbc.M412921200 PMID: 15741167

[16] Aoyagi T, Matsui T. Phosphoinositide-3 kinase signaling in cardiac hypertrophy and heart failure. Curr Pharm Des, 2011, 17(18):1818–1824. https://doi.org/10.2174/138161211796390976 PMID: 21631421 PMCID: PMC3337715

[17] D'Oria R, Schipani R, Leonardini A, Natalicchio A, Perrini S, Cignarelli A, Laviola L, Giorgino F. The role of oxidative stress in cardiac disease: from physiological response to injury factor. Oxid Med Cell Longev, 2020, 2020:5732956. https://doi.org/10.1155/2020/5732956 PMID: 32509147 PMCID: PMC7244977

[18] Crozatier B, Ventura-Clapier R. Inhibition of hypertrophy, *per se*, may not be a good therapeutic strategy in ventricular pressure overload: other approaches could be more beneficial. Circulation, 2015, 131(16):1448–1457. https://doi.org/10.1161/CIRCULATIONAHA.114.013895 PMID: 25901070

[19] Kazakov A, Hall R, Jagoda P, Bachelier K, Müller-Best P, Semenov A, Lammert F, Böhm M, Laufs U. Inhibition of endothelial nitric oxide synthase induces and enhances fibrosis. Cardiovasc Res, 2013, 100(2):211–221. https://doi.org/10.1093/cvr/cvt181 PMID: 23863197

[20] Taegtmeyer H, Golfman L, Sharma S, Razeghi P, van Arsdall M. Linking gene expression to function: metabolic flexibility in the normal and diseased heart. Ann N Y Acad Sci, 2004, 1015:202–213. https://doi.org/10.1196/annals.1302.017 PMID: 15201161

[21] Kolwicz SC Jr. Lipid partitioning during cardiac stress. Biochim Biophys Acta, 2016, 1860(10):1472–1480. https://doi.org/10.1016/j.bbalip.2016.03.028 PMID: 27040509

[22] Jarc E, Petan T. Lipid droplets and the management of cellular stress. Yale J Biol Med, 2019, 92(3):435–452. PMID: 31543707 PMCID: PMC6747940

[23] García-Rúa V, Otero MF, Lear PV, Rodríguez-Penas D, Feijóo-Bandín S, Noguera-Moreno T, Calaza M, Álvarez-Barredo M, Mosquera-Leal A, Parrington J, Brugada J, Portolés M, Rivera M, González-Juanatey JR, Lago F. Increased expression of fatty-acid and calcium metabolism genes in failing human heart. PLoS One, 2012, 7(6):e37505. https://doi.org/10.1371/journal.pone.0037505 PMID: 22701570 PMCID: PMC3368932

[24] Jain SS, Luiken JJFP, Snook LA, Han XX, Holloway GP, Glatz JFC, Bonen A. Fatty acid transport and transporters in muscle are critically regulated by Akt2. FEBS Lett, 2015, 589(19 Pt B):2769–2775. https://doi.org/10.1016/j.febslet.2015.08.010 PMID: 26296318

[25] Teunissen BEJ, Jongsma HJ, Bierhuizen MFA. Regulation of myocardial connexins during hypertrophic remodelling. Eur Heart J, 2004, 25(22):1979–1989. https://doi.org/10.1016/j.ehj.2004.08.007 PMID: 15541833

[26] Pinali C, Bennett HJ, Davenport JB, Caldwell JL, Starborg T, Trafford AW, Kitmitto A. Three-dimensional structure of the intercalated disc reveals plicate domain and gap junction remodeling in heart failure. Biophys J, 2015, 108(3):498–507. https://doi.org/10.1016/j.bpj.2014.12.001 PMID: 25650918 PMCID: PMC4317535

[27] Seidel T, Salameh A, Dhein S. A simulation study of cellular hypertrophy and connexin lateralization in cardiac tissue. Biophys J, 2010, 99(9):2821–2830. https://doi.org/10.1016/j.bpj.2010.09.010 PMID: 21044579 PMCID: PMC2965950

[28] Salas D, Puebla C, Lampe PD, Lavandero S, Sáez JC. Role of Akt aad Ca^{2+} on cell permeabilization *via* connexin43 hemichannels induced by metabolic inhibition. Biochim Biophys Acta, 2015, 1852(7):1268–1277. https://doi.org/10.1016/j.bbadis.2015.03.004 PMID: 25779082 PMCID: PMC4476395

[29] Cittadini A, Monti MG, Iaccarino G, Di Rella F, Tsichlis PN, Di Gianni A, Strömer H, Sorriento D, Peschle C, Trimarco B, Saccà L, Condorelli G. Adenoviral gene transfer of Akt enhances myocardial contractility and intracellular calcium handling. Gene Ther, 2006, 13(1):8–19. https://doi.org/10.1038/sj.gt.3302589 PMID: 16094411 PMCID: PMC2999753

[30] Sansbury BE, Riggs DW, Brainard RE, Salabei JK, Jones SP, Hill BG. Responses of hypertrophied myocytes to reactive species: implications for glycolysis and electrophile metabolism. Biochem J, 2011, 435(2):519–528. https://doi.org/10.1042/BJ20101390 PMID: 21275902 PMCID: PMC4072126

[31] Steinberg SF. Mechanisms for redox-regulation of protein kinase C. Front Pharmacol, 2015, 6:128. https://doi.org/10.3389/fphar.2015.00128 PMID: 26157389 PMCID: PMC4477140

[32] Ogawara Y, Kishishita S, Obata T, Isazawa Y, Suzuki T, Tanaka K, Masuyama N, Gotoh Y. Akt enhances Mdm2-mediated ubiquitination and degradation of p53. J Biol Chem, 2002, 277(14):21843–21850. https://doi.org/10.1074/jbc.M109745200 PMID: 11923280

[33] Spinale FG. Myocardial matrix remodeling and the matrix metalloproteinases: influence on cardiac form and function. Physiol Rev, 2007, 87(4):1285–1342. https://doi.org/10.1152/physrev.00012.2007 PMID: 17928585

[34] Wang X, Berry E, Hernandez-Anzaldo S, Takawale A, Kassiri Z, Fernandez-Patron C. Matrix metalloproteinase-2 mediates a mechanism of metabolic cardioprotection consisting of negative regulation of the sterol regulatory element-binding protein-2/3-hydroxy-3-methylglutaryl-CoA reductase pathway in the heart. Hypertension, 2015, 65(4):882–888. https://doi.org/10.1161/HYPERTENSIONAHA.114.04989 PMID: 25646300

[35] Parente JM, Castro MM. Matrix metalloproteinase in the cardiovascular remodeling of hypertension: current insights and therapeutic potential. Metalloproteinases Med, 2018, 5:1–11. https://doi.org/10.2147/MNM.S104793 https://www.dovepress.com/getfile.php?fileID=41491

[36] Iyer RP, Jung M, Lindsey ML. MMP-9 signaling in the left ventricle following myocardial infarction. Am J Physiol Heart Circ Physiol, 2016, 311(1):H190–H198. https://doi.org/10.1152/ajpheart.00243.2016 PMID: 27208160 PMCID: PMC4967202

[37] DeLeon-Pennell KY, Tian Y, Zhang B, Cates CA, Iyer RP, Cannon P, Shah P, Aiyetan P, Halade GV, Ma Y, Flynn E, Zhang Z, Jin YF, Zhang H, Lindsey ML. CD36 is a matrix metalloproteinase-9 substrate that stimulates neutrophil apoptosis and removal during cardiac remodeling. Circ Cardiovasc Genet, 2016, 9(1):14–25. https://doi.org/10.1161/CIRCGENETICS.115.001249 PMID: 26578544 PMCID: PMC4758866

Corresponding author

Gabriela Tanko, PhD, Department of Pathophysiology and Pharmacology, Nicolae Simionescu Institute of Cellular Biology and Pathology, 8 Bogdan Petriceicu Haşdeu Street, Sector 5, 050568 Bucharest, Romania; Phone +4021–319 45 18, e-mail: gabriela.tanko@icbp.ro

Received: November 3, 2020

Accepted: February 28, 2022